A simulation study of the disordered phase of CBr_4: II. Collective properties and rotation–translation coupling

Martin T Dove and Ruth M Lynden-Bell

Department of Theoretical Chemistry, University Chemical Laboratory, Lensfield Road, Cambridge CB2 1EW, UK

Abstract. Molecular dynamics simulation techniques have been used to study the orientationally disordered phase of carbon tetrabromide at 345 K, with particular emphasis placed on analysing the coupling between orientations and translations. The wave-vector dependence of this coupling has been calculated, showing that there are no couplings of any sort at $k = 0$, and that over the surface of the Brillouin zone boundary there is a strong coupling between the transverse acoustic modes and the orientational variables that order in the low-temperature phase. The phase transition is discussed within the context of this coupling. The collective dynamics have been studied by calculations of various correlation functions, which become long-lived when the orientational–translation coupling becomes strong. It is shown that a simple Mori theory that includes this coupling is able to reproduce the observed behaviour. In particular, it has been found that when the coupling is strong, the acoustic modes appear in a coherent inelastic neutron scattering experiment as quasi-elastic scattering with full width at half-maximum height of less than 0.03 THz.

1. Introduction

In recent years there has been a growing interest in a class of materials that are essentially stable intermediate phases between liquid and crystalline phases, namely orientationally disordered (OD) crystals. The behaviour of these systems shows similarities with paramagnetic disorder, with the molecular centre-of-mass positions lying on an ordered crystallographic lattice, which is usually cubic or hexagonal, but with disorder in the molecular orientations. Like the magnetic analogues these systems undergo phase transitions to low-temperature ordered phases, but the analogy is far from perfect. The forces in OD crystals are far more complex than Ising- or Heisenberg-type interactions, often yielding a delicate balance between forces that favour order (e.g. crystal fields) and others that oppose order (which might arise from steric hindrance interactions). Moreover, there generally exists in OD crystals a coupling between the orientational variables and the acoustic phonons which is often sufficiently strong to radically alter the nature of the collective excitations, and which plays an important role in the transitions to the ordered state. A theory of OD crystals that takes explicit account of this coupling, usually known as rotation–translation coupling, has been developed by Michel and Naudts (1977, 1978), and this theory has explained many of the static and dynamic properties of the OD phases and phase transitions in KCN, $NaNO_2$ (Michel 1981) and thiourea (Parlinski and Michel 1984).

In this paper we analyse the coupling between the orientational variables and the acoustic phonons in the OD phase of CBr_4, using the technique of molecular dynamics simulation (MDS). A realistic model inter-molecular potential was developed in the preceding paper (Dove 1986, referred to hereafter as I), and was used to study the single-molecule properties such as the distribution of molecular orientations and the reorientational dynamics.

The OD phase of CBr_4 exists over the temperature range 320–365 K, and has a face-centred cubic structure with the molecules lying on sites of O_h symmetry (Dolling *et al* 1979, More *et al* 1980). Both the OD phase and the low-temperature ordered structure have been previously studied using neutron and x-ray scattering techniques, and all relevant results are reviewed in I. We note here that the collective dynamics of the OD phase of CBr_4 have been studied experimentally by coherent inelastic neutron scattering (More *et al* 1980, 1984, More and Fouret 1980). Acoustic phonons have been observed, but with rapid weakening and broadening of the phonon peaks with increasing wave-vector, and quasi-elastic scattering was observed at many points in reciprocal space (see also More 1982). No librational (optic) modes could be observed.

The main conclusion of I was that the disorder and rotational dynamics of the OD phase of CBr_4 are more complex than previously thought. It had been suggested (e.g. by Coulon and Descamps 1980) that the molecules would in general have a D_{2d} orientation, of which there are six ways of orienting a tetrahedral molecule (see I for a description), with the molecules undergoing reorientational jumps between these discrete orientations. This gives a discrete spin model for the disorder. However, the results of I show that this model must be modified; instead the range of orientations is wider and the molecular motions consist of slow rotational diffusion interrupted by short periods of free spinning.

The rest of this paper follows this outline. In order to study the coupling between the orientational variables and the acoustic phonons we need to consider the collective properties of the systems. The formalism will be defined, and the wave-vector dependence of the static coupling will be analysed. We will then study the effect of this coupling on the collective dynamics, which can also be measured experimentally. These formal results will be incorporated into a Mori-type theory which will be used to describe the effects of the coupling on the correlation functions associated with the collective modes. Finally the phase transition to the ordered phase will be assessed in the light of these results.

2. Analysis method

2.1. Simulation details

Most of the technical details of the simulations are presented in I, and so we mention here only those features that are of direct importance to the present study. The calculations were performed on the ICL distributed array processor, which allows the use of samples with periodic boundary conditions and 4096 molecules. For reasons explained in detail elsewhere (Pawley and Thomas 1982) it is necessary to use triclinically-shaped samples. In the present case the shape of the MDS sample is defined by the three vectors

$$X = (10, -1, 0)a \qquad Y = (-2, 10.5, -0.5)a \qquad Z = (-2, -1, 10)a$$

where a is the length of the FCC unit cell, and the vectors are defined with respect to the

three orthogonal axes of the cubic unit cell. The corresponding reciprocal-lattice vectors are thus

$$X^* = (104.5, 21, 23)/1024a \qquad Y^* = (10, 100, 12)/1024a$$
$$Z^* = (0.5, 5, 103)/1024a$$

where we have followed the practice in crystallography of omitting factors of 2π. Any allowed reciprocal-lattice vector can be constructed as a linear combination of these three basis vectors. It is clear however that no such combination will give a vector that lies exactly along a symmetry direction, but in practice it is usually possible to find a combination that produces a vector lying close to a required vector. For example the vector Z deviates from the 001 direction by only 2.8°, and the sum of these three vectors deviates from the 111 direction by only 4.3°.

The inter-molecular potential used in this study is the $f = 0.75$ model of paper I. The potential is a sum of site–site Lennard–Jones interactions, with each molecule having four sites located three-quarters of the way along the C–Br bond. Only nearest- and next-nearest-neighbour interactions were included. The equations of motion appropriate for a microcanonical ensemble were used. The mean temperature and pressure were $\simeq 345$ K and $\simeq 0$ kbar respectively, and the unit cell size used was 8.85 Å. The simulation was carried out for 9730 time steps, which correspond to a simulated time length of 97.3 ps.

2.2. Essential formalism

This study is primarily concerned with the collective variables of the system, which are simply the Fourier transforms of the corresponding real-space variables. The variable for the acoustic phonons $u(k)$ is obtained from the set of displacements of the molecules $u(R_i)$ from their equilibrium lattice positions R_i, namely

$$u(k) = N^{-1/2} \Sigma u(R_i) \exp(ik \cdot R_i)$$

where N is the number of molecules and the summation is over all molecules, and k is the associated wave-vector. Similarly the velocity variable $\dot{u}(k)$ can be obtained from the molecular velocities $\dot{u}(R_i)$. The seven variables associated with the orientations $Y_\alpha(R_i)$ have been described in I as linear combinations of the $l = 3$ spherical harmonics, and are given as summations of unit vectors (x, y, z) along the C–Br bonds in table 1. In

Table 1. Definitions of the seven orientational variables expressed as sums over the four normalised C–Br bond vectors (x_i, y_i, z_i).

$Y_1 = \dfrac{3^{3/2}}{4} \sum_{i=1}^{4} x_i y_i z_i$	$Y_5 = \dfrac{3^{3/2}}{8} \sum_{i=1}^{4} z_i(x_i^2 - y_i^2)$
$Y_2 = \dfrac{3(5)^{1/2}}{40} \sum_{i=1}^{4} (5z_i^3 - 3z_i)$	$Y_6 = \dfrac{3^{3/2}}{8} \sum_{i=1}^{4} x_i(y_i^2 - z_i^2)$
$Y_3 = \dfrac{3(5)^{1/2}}{40} \sum_{i=1}^{4} (5x_i^3 - 3x_i)$	$Y_7 = \dfrac{3^{3/2}}{8} \sum_{i=1}^{4} y_i(z_i^2 - x_i^2)$
$Y_4 = \dfrac{3(5)^{1/2}}{40} \sum_{i=1}^{4} (5y_i^3 - 3y_i)$	

I it is shown that the values of the variables Y_5, Y_6 and Y_7 are associated with the D_{2d} symmetry orientations that order in the low-temperature phase. As for the displacement variables, associated collective variables can be obtained by Fourier transformation.

The dynamical properties of an ensemble of molecules are studied via correlation functions; for example we can describe a correlation function associated with the component of the displacement as $\langle u_\alpha(k, t)u_\alpha(-k, 0)\rangle$. Where different variables are coupled the cross-correlation functions will be non-zero. Of particular importance is the coupling between orientational and displacement variables, and formally this can be studied through the wave-vector-dependent parameter $\lambda_{\alpha\beta}(k)$ defined as (Lynden-Bell *et al* 1983)

$$\lambda_{\alpha\beta}(k) = \langle u_\alpha(k, 0)Y_\beta(-k, 0)\rangle/(\langle u_\alpha(k, 0)u_\alpha(-k, 0)\rangle^{1/2}\langle Y_\beta(k, 0)Y_\beta(-k, 0)\rangle^{1/2}).$$

It is clear that $|\lambda_{\alpha\beta}(k)| \leq 1$, and when $\lambda_{\alpha\beta}(k) = \pm 1$ the two variables are completely coupled and a phase transition is precipitated.

Of course, only variables with the same symmetry will be coupled. We give in table 2 the relevant linear combinations of the variables together with their symmetry types for the two symmetry directions we have studied.

3. Rotation–translation coupling

The coupling coefficient $\lambda_{\alpha\beta}(k)$ is shown in figure 1 as a function of wave-vector k for the symmetry directions 001 and 111. These coefficients are consistent with the symmetry analysis given in table 2, with no observed coupling between variables of different symmetry. We note the following features to emerge from figure 1.

Table 2. Relevant collective variables for symmetry points in reciprocal space with appropriate symmetry species. Only modes with the same symmetry will couple.

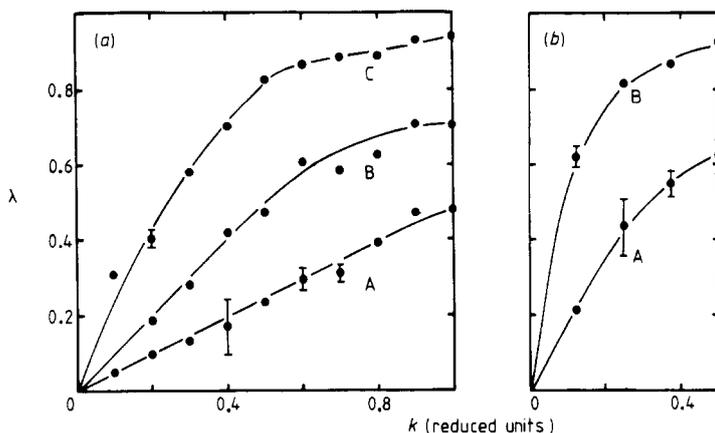|	Variable	Symmetry type
$k = 0$	u_x, u_y, u_z	T_{1u}
	Y_1	A_{2u}
	Y_2, Y_3, Y_4	T_{1u}
	Y_5, Y_6, Y_7	T_{2u}
$k = (00\xi)$	u_x, u_y	E
	u_z	A_1
	Y_1	B_2
	Y_3, Y_4	E
	Y_2	A_2
	Y_6, Y_7	E
	Y_5	B_1
$k = (\xi\xi\xi)$	$(u_x - u_y)/2^{1/2}, (u_x + u_y - 2u_z)/6^{1/2}$	E
	$(u_x + u_y + u_z)/3^{1/2}$	A_1
	Y_1	A_1
	$(Y_2 + Y_3 + Y_4)/3^{1/2}$	A_1
	$(Y_3 - Y_4)/2^{1/2}, (Y_3 + Y_4 - 2Y_2)/6^{1/2}$	E
	$(Y_5 + Y_6 + Y_7)/3^{1/2}$	A_2
	$(Y_6 - Y_7)/2^{1/2}, (Y_6 + Y_7 - 2Y_5)/6^{1/2}$	E

Figure 1. The rotation–translation coupling coefficient $\lambda_{\alpha\beta}(k)$. (*a*) Modes along the 001 direction. Curves A, B and C are for the TA mode coupled to T_{1u} orientation, the LA mode coupled to T_{1u} orientation, and the TA mode coupled to T_{2u} orientation, respectively. (*b*) Modes along the 111 direction. Curves A and B are for the TA mode coupled to T_{1u} and T_{2u} orientations respectively.

(i) In both symmetry directions the transverse acoustic (TA) modes, which are degenerate, couple to two orientational variables, one of which is from the T_{1u} set and the other from the T_{2u} set. The longitudinal acoustic (LA) mode in the 001 direction couples to one orientational variable, but in the 111 direction the LA mode does not couple to any variables although such coupling is not forbidden by symmetry.

(ii) In both symmetry directions the TA modes couples more strongly to the T_{2u} modes than to the T_{1u} modes. This observation is important in view of the fact that the orientations associated with the T_{2u} variables (the D_{2d} orientations of I) are the orientations that order in the low-temperature structure (More *et al* (1980); see also I), and as the phase transition involves a change in the shape of the unit cell it is clear that the transition is associated with a coupling between the orientational variables and the acoustic phonons. In I it was shown that the D_{2d} spin model, in which all molecules are only oriented in one of the D_{2d}-type orientations, is too severe, and that instead the molecules have a wider range of continuously changing orientations. However, it was shown that there exists an incipient ordering of these orientations, and in figure 1 this incipient ordering is even more strongly revealed through the large rotation–translation coupling.

(iii) The coupling parameters reach their maximum values at the Brillouin zone boundary points in both symmetry directions, and are all zero at the zone centre. This is the opposite behaviour to that found in NaCN (Lynden-Bell *et al* 1983), where the maximum coupling was at the zone centre and the coupling vanished at the zone boundary because of symmetry constraints. It can be seen from table 2 that the coupling coefficient associated with the T_{2u} orientational variables should go to zero at the zone centre for symmetry reasons. Although the second coefficient is allowed to have a non-zero value at the zone centre, there is no coupling to acoustic modes at $k = 0$ as they correspond to uniform displacements. Unlike the case of KCN, the ordering phase transition is not accompanied by a ferroelastic distortion. Of importance is the fact that the coupling coefficient associated with the T_{2u} orientational variables is close to unity

at the zone boundary. It is clear from the definition of λ that a value of unity corresponds to complete correlation of the orientational and phonon variables, which would precipitate a phase transition. This is consistent with the current theories of rotation–translation coupling (Michel and Naudts 1977, 1978), which show that strong couplings cause the acoustic phonon frequencies to soften and the mode to become unstable. The simulation sample is thus close to undergoing a phase transition associated with the ordering of the T_{2u} orientational variables, which is probably not surprising since in Nature the disordered phase exists over a narrow temperature range (45 K) compared with the high-transition point (320 K).

The phase transition can be considered as a two-stage process (Pick 1984). The molecular positions do not differ much from those of a FCC lattice but the monoclinic super-cell can be thought of as arising from an instability at the zone-boundary point in one of the 111 symmetry directions, followed by a second instability at a point half-way to the zone boundary along one of the other 111 directions. This transition pathway is consistent with the form of the associated $\lambda(k)$ shown in figure 1: the maximum is at the zone boundary, but in addition $\lambda(k)$, rises steeply from the zone-centre point towards a large value at the point half-way to the zone boundary, with a much flatter variation with k in the region from $(\frac{1}{4} \frac{1}{4} \frac{1}{4})$ to $(\frac{1}{2} \frac{1}{2} \frac{1}{2})$. However, similar behaviour is also found along the 001 direction. This probably implies that there are a number of incipient instabilities in the OD phase, with the observed ordered phase having a slightly lower free energy than all other possible low-temperature structures. It is not surprising that this should be so, in view of the very delicate balance of competing interactions present and the complexity of the stable ordered structure.

4. Collective dynamics

As stated in § 2.2 we have constructed a number of time correlation functions, the relevant ones being

$$U_{\alpha\alpha}(k, t) = \langle u_\alpha(k, t) u_\alpha(-k, 0) \rangle$$

$$Y_{\alpha\beta}(k, t) = \langle Y_\alpha(k, t) Y_\beta(-k, 0) \rangle$$

$$C_{\alpha\beta}(k, t) = \langle u_\alpha(k, t) Y_\beta(-k, 0) \rangle.$$

The cross-correlation functions $C_{\alpha\beta}(k, t)$ are non-zero where there is a static coupling between the phonon and orientational variables given by $\lambda_{\alpha\beta}(k)$ (§ 3), and the orientational correlation functions $Y_{\alpha\beta}(k, t)$ are non-zero for all $\alpha = \beta$ and for $\alpha \neq \beta$ where the variables $Y_\alpha(k)$ and $Y_\beta(k)$ are of the same symmetry. The existence of a coupling between the two different orientational variables that couple to the same acoustic phonon is expected, if only via their coupling to the phonon.

Experimentally, the collective dynamics of a solid or liquid would be studied by coherent inelastic neutron scattering, which probes the correlation function associated with density fluctuations through measurements of the inelastic scattering function $S(Q, \omega)$:

$$S(Q, \omega) = \int \langle \rho(Q, t) \rho(-Q, 0) \rangle \, e^{i\omega t} \, dt$$

where Q is the wave-vector transfer of the neutron beam ($= $Bragg vector $\pm k$). The

density operator $\rho(\boldsymbol{Q}, t)$ is given by

$$\rho(\boldsymbol{Q}, t) = \sum_i b_i \exp(\mathrm{i}\boldsymbol{Q} \cdot \boldsymbol{r}_i)$$

where r_i is the position of the ith atom and b_i is the scattering length of that atom. Formally $S(\boldsymbol{Q}, \omega)$ gives the neutron scattering intensity as a sum of single- and multiple-phonon scattering processes, whereas in general a neutron scattering experiment will be designed to observe the one-phonon scattering in the most favourable experimental configuration since this gives most information (phonon frequencies, lifetimes, dispersion etc). The correlation functions $U_{aa}(\boldsymbol{k}, t)$ etc are essentially those probed by single-phonon scattering, and in the Appendix we show the relationship between these correlation functions and the one-phonon inelastic scattering function. However, we will mainly concentrate on the time correlation functions rather than their Fourier transforms.

We point out at the outset that there are problems in the study of dynamics that are associated with the use of periodic boundary conditions which have been discussed in some detail by Dove *et al* (1986). In summary, a propagating fluctuation will travel through the periodic boundaries and interact with itself after a time delay. The smallest such time delay is given by the period of the longitudinal acoustic mode with the lowest allowed wave-vector, which defines a critical time for the analysis of correlation functions; correlation functions can only be considered reliable for times less than this critical time. In the present case the period of the lowest-k LA mode in the 111 direction is $\simeq 2$ ps. Although there will be no harmonic coupling between this mode and other modes, there will nevertheless almost certainly be some anharmonic effects that cannot be ignored. This feedback effect causes problems when it is intended to study the Fourier transform of a correlation function as good resolution in the frequency domain requires long times in the correlation function, and for this reason we leave this aspect of the work to the next section. Of course, there is no problem if the correlation function has significantly decayed in a time less than the critical time, which is the case with some of the variables.

We consider the behaviour of the time correlation functions for three cases.

4.1. Variables that do not couple to any others

Here we consider the LA variable in the 111 direction and some of the orientational variables. The LA variable is shown for each wave-vector in figure 2. The behaviour is that of a well defined normal mode that increases in frequency but becomes more damped on increasing k. This mode has been observed by coherent inelastic scattering by More and Fouret (1980), and it was found to have the same k-dependence as outlined above, with the phonon peaks becoming weaker and broader with increasing k. As there is no coupling of this mode to an orientational variable, this damping must arise from anharmonic interactions and dynamic coupling to the orientational disorder. We should remark that More and Fouret have used their data on this mode to fit an expression for $S(\boldsymbol{Q}, \omega)$ with rotation–translation coupling (Michel and Naudts 1978). They obtained a good fit to data for $\boldsymbol{k} = (0.1, 0.1, 0.1)$ with a value of an undefined coupling parameter of 0.8, despite the fact that the model expression was inappropriate in this case as this mode does not directly couple to any orientational variable in this symmetry direction.

On the other hand, the orientational variables that do not couple to the phonons show little k-dependence. In general, the decaying orientational correlation functions
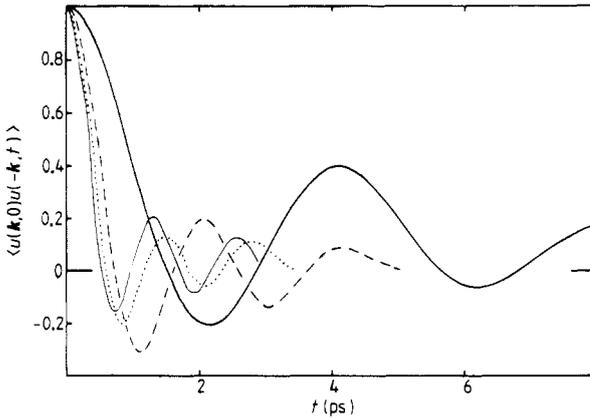
Figure 2. The LA mode correlation function $\langle u(\mathbf{k}, 0)u(-\mathbf{k}, t)\rangle$ along the 111 direction. The reduced wave-vectors are $(\frac{1}{8}, \frac{1}{8}, \frac{1}{8})$ (heavy curve), $(\frac{1}{4}, \frac{1}{4}, \frac{1}{4})$ (broken curve), $(\frac{3}{8}, \frac{3}{8}, \frac{3}{8})$ (dotted curve) and $(\frac{1}{2}, \frac{1}{2}, \frac{1}{2})$ (fine curve).
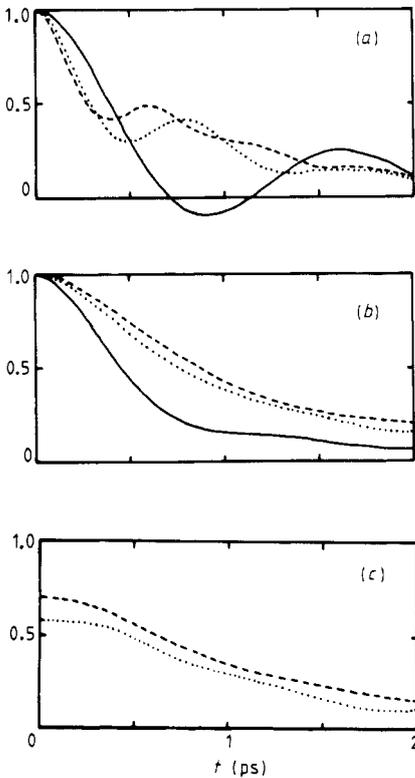

Figure 3. Correlation functions for LA T_{1u} coupling along the 001 direction. (*a*) The displacement–displacement correlation function. (*b*) The orientation–orientation correlation function. (*c*) The cross-correlation function. Full, dotted and broken curves refer to the reduced wave-vectors $(0, 0, 0.3)$, $(0, 0, 0.6)$ and $(0, 0, 1)$ respectively.

are either approximately gaussian-like (A_{2u}, T_{1u}) or exponential-like (T_{2u}) in form, with half-widths at half-maximum height of 1 ps or less.

4.2. Variables with LA mode coupling

In the 001 direction the LA mode couples to the orientational variable Y_2, with the coupling parameter reaching a maximum value of 0.7 (figure 1). As this is not as strong as for the TA modes (see below), it is unlikely that this coupling is connected with the phase transition. The behaviour of the time correlation functions $U_{33}(k, t)$ and $Y_{22}(k, t)$ are shown in figure 3. $U_{33}(k, t)$ behaves as the corresponding correlation function in the 111 direction, showing a normal-mode behaviour that becomes damped with increasing wave-vector. The orientational correlation function is seen to broaden by a factor of two on increasing k from the zone centre to the zone boundary but otherwise remains the same across the Brillouin zone. Also shown in figure 3 is the cross-correlation function $C_{32}(k, t)$. This is similar to $Y_{22}(k, t)$ in structure, and similarly does not vary much other than in amplitude. In the low-k regime the amplitude is not much greater than the noise and so the correlation function is ill defined in the simulations.

4.3. Variables with TA mode coupling

The correlation functions for variables that couple to the TA variables are the ones that are of most interest. These exist in both the 001 and 111 symmetry directions, and representative correlation functions for a number of wave-vectors are shown in figures 4 and 5 respectively. Because one of the coupling coefficients in each direction approaches unity (figure 1) the effects of the coupling are more dramatic than in the previous case. As has also been stressed in § 3, the displacement variables couple to two orientational variables, so in each direction we must consider the behaviour of six correlation functions, four of which are shown in figures 4 and 5. At low k, where the coupling is
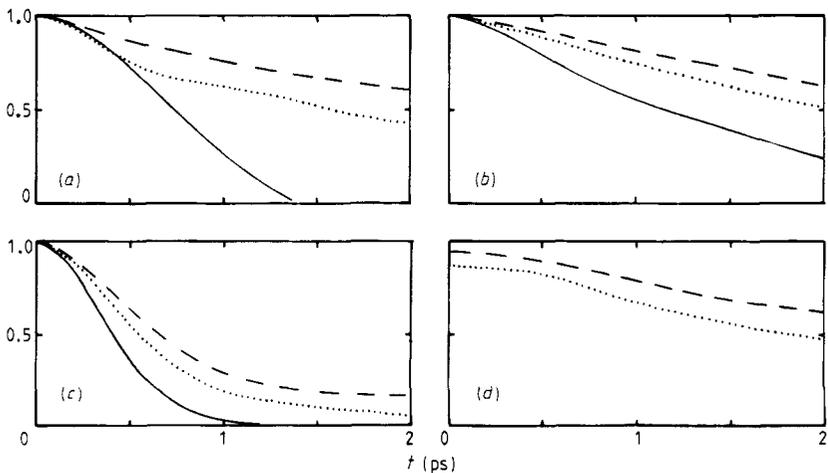

Figure 4. Correlation functions for TA orientation coupling along the 001 direction. (*a*) The displacement–displacement correlation functions. (*b*) The T_{2u} orientation–orientation correlation function. (*c*) The T_{1u} orientation–orientation correlation function. (*d*) The T_{2u} cross-correlation function. Full, dotted and broken curves refer to the reduced wave-vectors $(0, 0, 0.3)$, $(0, 0, 0.6)$ and $(0, 0, 1)$ respectively.
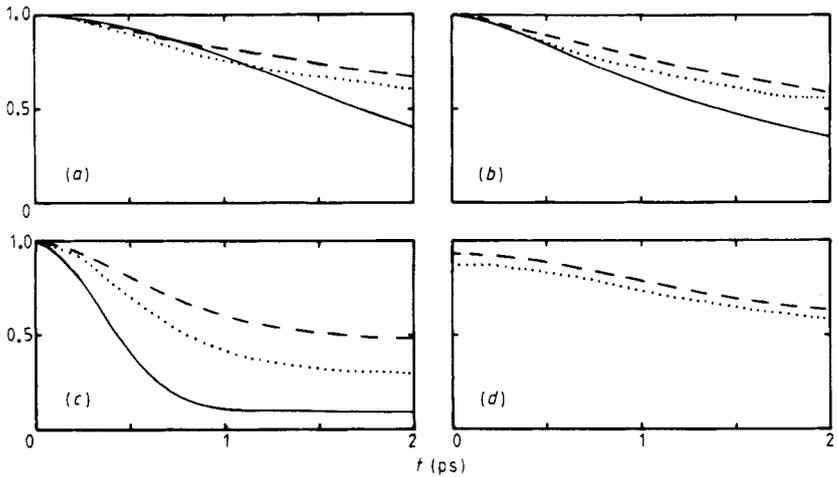
Figure 5. As for figure 4, but along the 111 direction. Here the full, dotted and broken curves refer to the reduced wave-vectors $(\frac{1}{4}, \frac{1}{4}, \frac{1}{4})$, $(\frac{3}{8}, \frac{3}{8}, \frac{3}{8})$ and $(\frac{1}{2}, \frac{1}{2}, \frac{1}{2})$ respectively.

small, the displacement variable correlation functions correspond to normal modes which, presumably because of anharmonic effects, become heavily damped on increasing wave-vector. The orientational correlation functions show the two types of behaviour discussed in case (i), depending on whether they are the T_{1u} or T_{2u} variables. However, as k increases beyond the low-k regime the various wave-vector-dependent coupling parameters increase, and the effects of the coupling are seen in the various correlation functions. Thus on increasing k the TA correlation functions become more relaxational in character rather than being damped oscillations, with widths that increase with k. The orientational correlation functions and the cross-correlation functions similarly increase in lifetime with increasing k. In the strong-coupling limit the three relevant correlation functions become very similar in form and lifetimes. Experimentally, this would be seen in the narrowing in the frequency domain of quasi-elastic coherent neutron scattering on approaching the critical points in the Brillouin zone at appropriate points in reciprocal space.

4.4. Comparison with experimental data

Some coherent inelastic neutron scattering data from the OD phase of CBr_4 are available (More and Fouret 1980, More 1982, More *et al* 1984), but unfortunately they cannot be considered to be extensive. Essentially the data represent two aspects of the collective dynamics: studies of the acoustic modes in the low-wave-vector limit, and measurements of widths of quasi-elastic scattering peaks in the vicinity of the strong anomalous diffuse scattering peak (More *et al* 1980).

The frequencies of the acoustic modes in the 001 and 111 directions have been measured by coherent inelastic scattering in a 'constant-energy' experiment (More and Fouret 1980). Results for the phonon wave-vector at selected frequencies for both experiment and similation are given in table 3. The calculated frequencies have either been obtained from the oscillations in the correlation function $U_{\alpha\alpha}(k, t)$ or indirectly from the standard quasi-harmonic result (see, e.g., Cowley 1980):

$$\nu^2(k) = k_B T / (4\pi m \langle u_\alpha(k) u_\alpha(-k) \rangle).$$

Table 3. Reduced phonon wave-vectors for acoustic phonons at constant frequency for the two symmetry directions (001) and (111). The upper and lower parts of the table are results from experiments (More and Fouret 1980) and simulation respectively.

Frequency (THz)	$k_{LA}(111)$	$k_{TA}(111)$	$k_{LA}(001)$	$k_{TA}(001)$
0.1	0.044	0.086	0.071	0.153
0.2	0.073	0.164	0.118	0.305
0.4	0.134	0.298	0.210	0.611
0.1	0.025	0.086	0.070	0.106
0.2	0.049	†	0.131	0.206
0.4	0.101	†	0.261	†

† Inapplicable as the acoustic phonon has softened below this frequency.

The calculated dispersion curves are given in figure 6. The most striking point is that the TA modes soften considerably towards the zone boundary. As this effect is not indicated in the data presented by More and Fouret (1980), complete comparison in table 3 is not possible. Nevertheless, the agreement between calculated and measured frequencies, particularly at low k, is satisfactory, the main discrepancies being that the calculated TA modes soften at lower wave-vectors than apparently observed experimentally. On the other hand, More and Fouret (1980) highlight an apparent softening of the velocity of sound at the zone centre, about which the simulations are unable to give any information. Since the rotation–translation coupling approaches zero at this point, some other mechanisms must be responsible for any softening. Moreover, the apparent extent of this softening is much less than in crystals with a true elastic softening (e.g. KCN, Rowe *et al* (1975); s-triazine, Dove *et al* 1983).

More *et al* (1984) have measured quasi-elastic scattering at a number of points in reciprocal space, observing lorentzian scattering profiles with half-widths at half-maximum height in the range 0.03–0.05 THz. This suggests the existence of relaxation collective fluctuations of the form $e^{-t/\tau}$, where the relaxation time τ is of the order of 3–5 ps. This relaxation time is consistent with the relaxation times for some of the correlation functions shown in figures 4 and 5. However, the experimentally determined
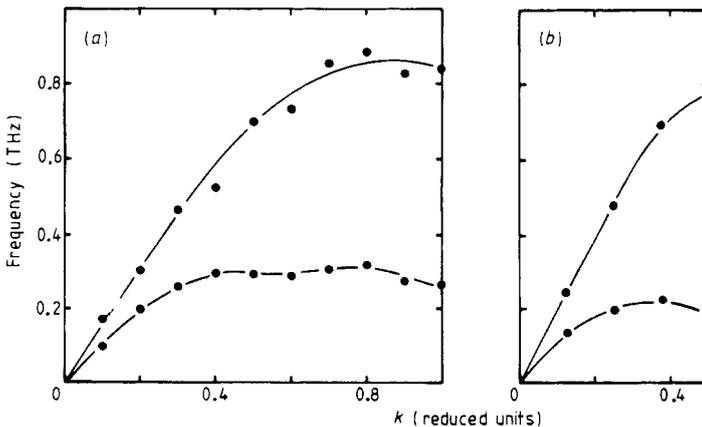

Figure 6. Acoustic phonon dispersion curves in the 001 direction (*a*) and 111 direction (*b*). The upper curves are for the LA modes, and the curves are drawn as guides to the eye.

relaxation times did not vary with k as much as was observed in this simulation study, a point that we discuss later.

5. Analysis of the effect of coupling on the dynamics

It is the purpose of this section to tie together the results of the two previous sections in order to analyse more generally the effect that rotation–translation coupling has on the dynamics of the OD phase of CBr_4. In order to do this we follow the work of Michel and Naudts (1978) and Lynden-Bell *et al* (1983) and employ a Mori-type formalism. In this section we develop the relevant equations of motion and assess the extent to which the theory together with parameters extracted from the simulations gives a realistic representation of the calculated correlation functions. Finally, with the assumption that the Mori theory at least qualitatively contains the essential physics of the problem, we use the theory in an exploratory manner to explain the overall effects of the coupling.

The essence of this approach is that a set of dynamical variables expressed as a vector $V(t)$ obey a simple equation of motion:

$$dVt/dt = (\Omega - R)V(t)$$

where Ω is a restoring force matrix and R is a relaxation matrix. In our analysis we follow Michel and Naudts (1978) and construct the elements of vector $V(t)$ as linear combinations of the variables $u_\alpha(k, t)$, $\dot{u}_\alpha(k, t)$, $Y_\beta(k, t)$ and $Y_\gamma(k, t)$, the only difference being that we now have to consider two orientational variables instead of just one. In order that the components of V are all orthogonal and normalised, we define

$$V_1(t) = u_\alpha(k, t)/\langle u_\alpha(k, 0)u_\alpha(-k, 0)\rangle^{1/2}$$

$$V_2(t) = \dot{u}_\alpha(k, t)/\langle \dot{u}_\alpha(k, 0)\dot{u}_\alpha(-k, 0)\rangle^{1/2}$$

$$V_3(t) = [Y_\beta(k, t)/\langle Y_\beta(k, 0)Y_\beta(-k, 0)\rangle^{1/2} - \lambda_{\alpha\beta}V_1(t)]\alpha_3^{-1}$$

$$V_4(t) = [Y_\gamma(k, t)/\langle Y_\gamma(k, 0)Y_\gamma(-k, 0)\rangle^{1/2} - \lambda_{\alpha\beta}V_1(t) - \gamma V_3(t)]\alpha_4^{-1}$$

where

$$\alpha_3 = (1 - \lambda_{\alpha\beta}^2)^{1/2} \qquad \alpha_4 = (1 - \lambda_{\alpha\gamma}^2 - \gamma^2)^{1/2}$$

and

$$\gamma = [\langle Y_\beta(k, 0)Y_\gamma(-k, 0)\rangle/\langle Y_\beta(k, 0)Y_\beta(-k, 0)\rangle^{1/2}\langle Y_\gamma(k, 0)Y_\gamma(-k, 0)\rangle^{1/2} - \lambda_{\alpha\beta}\lambda_{\alpha\gamma}]\alpha_3^{-1}.$$

The equation for $V(t)$ can be solved by diagonalisation of the matrix $(\Omega - R)$, and the correlation functions of interest (§ 4) can be easily constructed as linear combinations of the correlation functions $V_x(t)V_y(0)$.

The restoring force matrix Ω is assumed to contain the harmonic restoring forces, and with the variables above is given by

$$\Omega = \begin{bmatrix} 0 & \omega_\alpha & 0 & 0 \\ -\omega_\alpha & 0 & \lambda_{\alpha\beta}\omega_\alpha/\alpha_3 & \gamma\omega_\alpha/(\alpha_3\alpha_4) \\ 0 & -\lambda_{\alpha\beta}\omega_\alpha/\alpha_3 & 0 & 0 \\ 0 & -\gamma\omega_\alpha/(\alpha_3\alpha_4) & 0 & 0 \end{bmatrix}$$

where

$$\omega_\alpha = \langle \dot{u}_\alpha(\mathbf{k}, 0)\dot{u}_\alpha(-\mathbf{k}, 0)\rangle^{1/2}/\langle u_\alpha(\mathbf{k}, 0)u_\alpha(-\mathbf{k}, 0)\rangle^{1/2}$$

$$= (k_B T/m)^{1/2}/\langle u_\alpha(\mathbf{k}, 0)u_\alpha(-\mathbf{k}, 0)\rangle^{1/2}$$

and T and m are the temperature and molecular mass respectively. We assume that the relaxation matrix has only three non-zero values: R_{22}, R_{33} and R_{44}. The latter two correspond to the damping of the orientational variables which represents the continuous rotational diffusion of the molecules, and R_{22} absorbs all effects of anharmonicities on the acoustic modes. Michel and Naudts (1978) and de Raedt and Michel (1980) neglect this term in their analysis of the OD phase of KCN, and although Lynden-Bell *et al* (1983) included it in their study of NaCN they found the appropriate value of R_{22} to be small compared with R_{33}. In the present case, however, such a term is necessary as it is clear that there is significant decay of all acoustic modes through anharmonic effects. In principle one should expect that other elements of the matrix **R** should be non-zero, which would represent relaxation effects on the acoustic modes and the orientations because of the orientation disorder, but in practice it is easier to assume that all such effects can be subsumed into appropriate values of the diagonal components. Moreover, the neglect of the orientational cross-terms Ω_{34} and R_{34} can be justified as in practice the value of γ is very small (see below).

In order to solve the differential equations for V we have used the values for ω_α, λ and γ as obtained from the simulations for different values of wave-vector $\mathbf{k}$ and described in previous sections. The only datum we have not given previously is the k-dependence of the static correlation function

$$\eta_{\beta\gamma}(\mathbf{k}) = \langle Y_\beta(\mathbf{k}, 0)Y_\gamma(-\mathbf{k}, 0)\rangle/\langle Y_\beta(\mathbf{k}, 0)Y_\beta(-\mathbf{k}, 0)\rangle^{1/2}\langle Y_\gamma(\mathbf{k}, 0)Y_\gamma(-\mathbf{k}, 0)\rangle^{1/2}$$

which we show in figure 7. Also in this figure we show the function $\lambda_{\alpha\beta}(\mathbf{k})\lambda_{\alpha\gamma}(\mathbf{k})$ for the
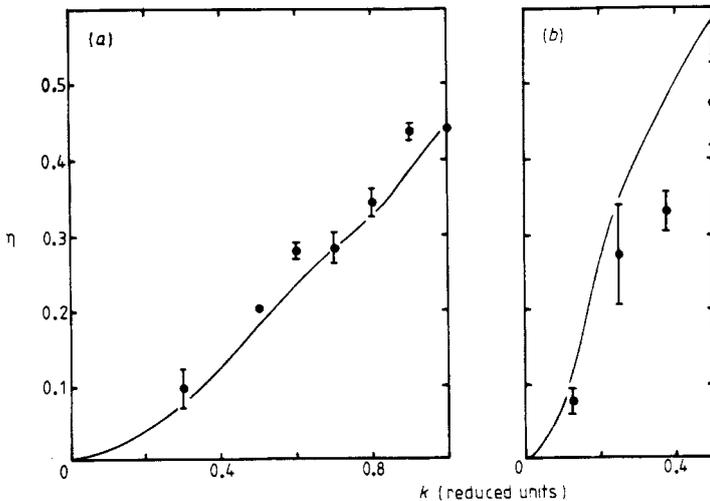

Figure 7. Static cross-orientation correlation functions

$$\eta_{\alpha\beta}(\mathbf{k}) = \langle Y_\alpha(\mathbf{k}, 0)Y_\beta(-\mathbf{k}, 0)\rangle/\langle Y_\alpha(\mathbf{k}, 0)Y_\alpha(-\mathbf{k}, 0)\rangle^{1/2}\langle Y_\beta(\mathbf{k}, 0)Y_\beta(-\mathbf{k}, 0)\rangle^{1/2}$$

for the 001 (*a*) and 111 (*b*) directions, for the variables Y_α and Y_β associated with the T_{1u} and T_{2u} sets of table 1. Circles show simulation data, and the curves are the functions $\lambda_\alpha(\mathbf{k})\lambda_\beta(\mathbf{k})$.

acoustic mode variable $u_\alpha(k)$ which couples to both $Y_\beta(k)$ and $Y_\gamma(k)$. It can be seen that the two functions are indistinguishable for the 001 direction and are very similar for the 111 direction. Hence it is clear that γ is always close to zero. The remaining three variables R_{22}, R_{33} and R_{44} were obtained from fitting the correlation functions obtained from the solution of V to the six correlation functions given in § 4.3. Because of the uncertainties caused by the use of periodic boundary conditions we limited the analysis of the correlation functions to data for less than 2 ps. The values of the fitted parameters, together with the variance between the fitted and observed correlation functions are given in table 4. Representative functions are shown in figure 8. In general the agreement

Table 4. Results of fitting the Mori theory model to the correlation functions in the two symmetry directions. The last column gives the variance for the fits.

Reduced wave-vector	ω	λ_1	λ_2	η	R_{22}	R_{33}	R_{44}	Variance of fit
[001]								
0.1	0.603	0.230	0.040	0.012	0.0985	0.5001	2.5071	0.0039
0.2	1.232	0.430	0.090	0.043	0.5602	0.8274	2.3945	0.0040
0.3	1.634	0.577	0.133	0.090	0.9687	1.0264	2.1677	0.0032
0.4	1.847	0.698	0.182	0.145	1.5336	1.1435	1.9687	0.0017
0.5	1.835	0.825	0.230	0.207	2.0342	1.5803	1.8570	0.0013
0.6	1.810	0.865	0.276	0.218	2.1351	1.5482	1.6443	0.0016
0.7	1.910	0.885	0.320	0.325	2.8182	1.7286	1.4731	0.0010
0.8	1.992	0.885	0.390	0.372	2.9550	1.7261	1.6741	0.0028
0.9	1.715	0.928	0.470	0.410	1.9811	1.9095	1.8324	0.0015
1.0	1.652	0.938	0.480	0.440	2.7620	2.3669	1.7297	0.0011
[111]								
0.125	0.848	0.620	0.212	0.078	1.1372	0.9506	1.9550	0.0027
0.25	1.241	0.815	0.433	0.222	2.5981	1.4602	1.4108	0.0016
0.375	1.414	0.868	0.549	0.365	3.1252	1.9952	1.4899	0.0010
0.5	1.225	0.925	0.623	0.472	1.0590	2.5305	0.9939	0.0014

between the observed and calculated correlation functions is reasonable, although the fitted values of the relaxation parameters vary somewhat erratically with wave-vector. Nevertheless, the parameters do show a marked trend. It can be seen from figure 8 that the model fits least well to the T_{1u}-type orientation modes, which are the modes that couple less to the acoustic modes. It is clear that these correlation functions show a more complicated behaviour than the simple relaxational decay of the model, and possibly point to the necessity to use a time-dependent relaxation force or to include Y among the slow variables in the Mori theory. A frequency-dependent coefficient has been incorporated into a model for KCN by de Raedt and Michel (1980), but such a degree of sophistication was considered to be inappropriate here when the effects of other approximations (e.g. the total absorption of anharmonic effects into simple relaxation parameters and the neglect of off-diagonal relaxation effects) may be of comparable importance. On the other hand, the model reproduces the acoustic mode behaviour, the T_{2u} orientational correlation functions and the cross-correlation functions extremely well, although there still remain slight discrepancies as seen for the T_{1u} orientational correlation functions. Of particular note is the fact that the model correctly reproduces the feature that the correlation functions become relaxational and longer-lived as the rotation–translation coupling coefficient increases towards unity. This includes the
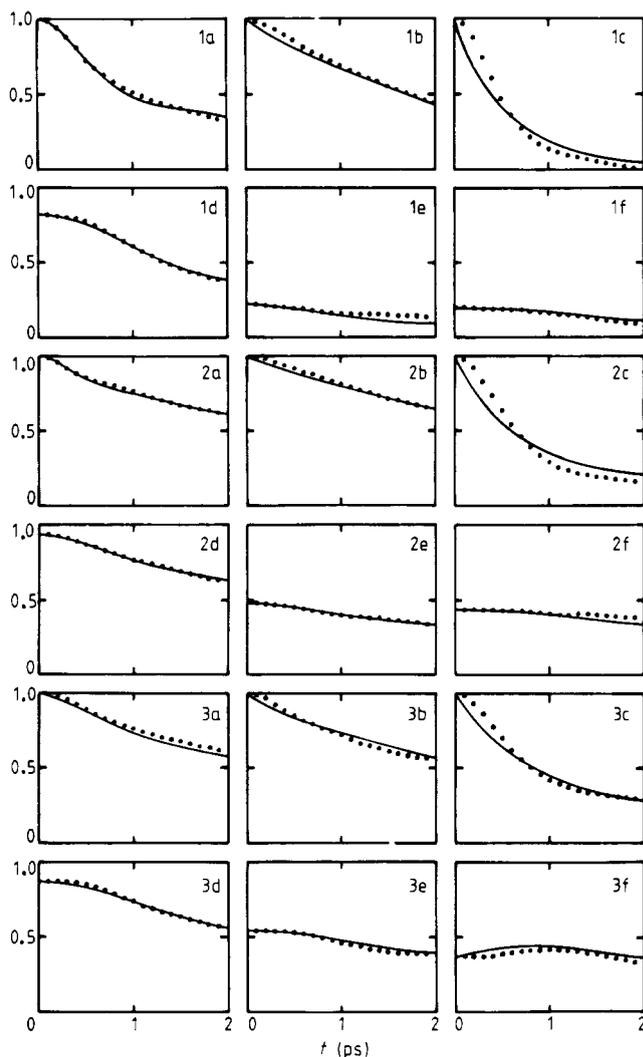
Figure 8. Representative correlation functions calculated using the Mori theory (full curves) as obtained by fitting to the simulation data (full circles). 1, 2 and 3 refer to the reduced wave-vectors $(0, 0, 0.5)$, $(0, 0, 1)$ and $(0.5, 0.5, 0.5)$ respectively. The different functions are (a) TA displacement–displacement; (b) T_{2u} orientation–orientation; (c) T_{1u} orientation–orientation; (d) T_{2u} orientation–displacement cross-term; (e) T_{1u} orientation–displacement cross-term; (f) T_{1u}–T_{2u} orientation cross-term.

acoustic mode correlation functions, which with increasing wave-vector (and hence coupling coefficient) change from oscillatory to relaxational behaviour. That this behaviour in the model does not simply result from the fitting procedure is seen in the fact that the fitted values of the relaxation coefficients (table 4) increase with increasing wave-vector, opposing the trend towards the slower relaxational behaviour. We conclude that at least qualitatively the Mori theory applied here provides a reasonable description of the behaviour observed in the simulations, with the discrepancies being understood within the approximations used. These approximations affect only the fine detail (mainly in the limit of $t \rightarrow 0$) and do not affect the overall behaviour.

Having established that the theory is a reasonable description of the behaviour of the dynamic properties of the OD phase of CBr_4, we summarise here the main features that the model reproduces. These have been confirmed by using the freedom to chose any value for any parameter. In the limit of small coupling, the acoustic mode is oscillatory (phonon-like) and the orientational modes are relaxational-like. In the absence of phonon damping ($R_{22} = 0$), the increase of rotation–translation coupling causes the acoustic phonon to become more relaxational, and the decay of the relaxational phonon and the orientational modes becomes slower as the coupling increases, even when the relaxational coefficients R_{33} and R_{44} remain constant. In the large-coupling regime the displacement and orientational correlation functions decay with similar characteristic times. The behaviour of the acoustic modes that do not couple to the orientational variables (see figure 2) shows that relaxational processes are an important part of the dynamic behaviour. Adding these to the model via a non-zero value of R_{22} smooths out residual fine detail (e.g. superimposed oscillations) on the phonon correlation functions, in accord with the observed correlation functions.

The phenomena of rotation–translation coupling has been studied in depth theoretically mainly for the alkali cyanides (Michel and Naudts 1977, 1978, Lynden-Bell *et al* 1983). The case of CBr_4 is more complicated in three regards. Firstly there are now two orientational variables that couple to the acoustic modes and that must be taken account of. Much of the analysis of the dynamics in KCN focuses on those symmetry directions for which only one mode is coupled. Secondly, the phonon frequencies ω are generally of the same size as either or both of the two relaxation frequencies R_{33} and R_{44}. Thus neither of the two limiting cases discussed by Michel and Naudts (1978) ($\omega \gg R$ or $\omega \ll R$), which have well defined behaviour, are relevant here. Thirdly there is a strong phonon damping in the present case, which to date has always been neglected (Powell *et al* 1983, Lynden-Bell *et al* 1983, Rowe *et al* 1978). Thus it is clear that in the application of the theory of rotation–translation coupling it is important to take careful note of the subtleties of the case in hand!

Experimentally these correlation functions can be studied through coherent inelastic neutron scattering (see the Appendix), where the scattering cross section is related to
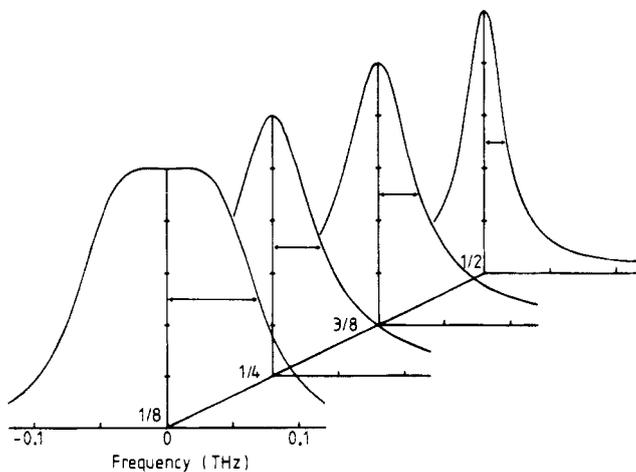

Figure 9. Fourier transforms of the TA displacement–displacement correlation functions (calculated from Mori theory) along the 111 direction. The values $\frac{1}{8}, \frac{1}{4}, \frac{3}{8}, \frac{1}{2}$ are to indicate the reduced wave-vector.

the time Fourier transforms of these functions. We consider here the scattering from the acoustic modes, which experimentally can be selected by using appropriate momentum transfers. Because of the problems encountered when considering long-time behaviour in the simulations (§ 4) we have used the correlation functions generated by the Mori theory. Fourier transforms for the TA modes propagating along the 111 direction are shown in figure 9. At the lowest wave-vector some structure can be seen in the scattering function, corresponding to scattering centred on zero frequency with two unresolved broad peaks at non-zero frequencies either side of zero frequency. However, at larger wave-vectors the scattering consists primarily of quasi-elastic scattering, with the width of the scattering function becoming more narrow as the coupling coefficient increases.

6. Discussion

6.1. Potential model

We comment, as in I, that in the few cases where it has been possible to compare the results of the simulations with experimental data the two sets of results have been in reasonable agreement. This gives confidence in the realism of the model we have developed, particularly as the model was parametrised using only two pieces of information concerning static averages. The potential model has now been tested over a wide range of independent static and dynamic properties.

6.2. The phase transition

One of the main results of I was to show that a model of the OD in CBr₄, in which each molecule was 'randomly' oriented with any of the six orientations of the low-temperature phase with frequent reorientations between different orientations whilst taking account of steric hindrance effects, gave an over-simplified description. The appeal of this model was that it enabled a fairly straightforward explanation of the phase transition to be given. However, in I it was shown that the single-molecule correlation functions for the variables associated with these orientations decayed more slowly than those for variables associated with other orientations. This implies that there exists an incipient orientational ordering in the OD phase, although somewhat hidden in the disorder! This observation has been confirmed in this study through the calculations of the coupling between the relevant orientational variables and TA modes, and as a result of this coupling the collective relaxational mode associated with the ordering orientation becomes very long-lived in the vicinity of the wave-vector at which the phase transition instability exists. The large slowly decaying fluctuations in these variables are precursors of the ordered phase.

That the OD is more complicated than the simple spin model is probably related to two features observed in this study. Firstly, the apparent instability at the zone boundary in the 001 direction indicates that there are a number of competing ordering processes, with the observed low-temperature ordered phase having a slightly lower free-energy minimum than other possible phases. This is not at all improbable. Secondly, the acoustic mode that couples to the ordering orientational variable also couples to another variable. Hence one expects the existence of other types of orientations in the OD phase. Alternatively one can consider certain complicating features of the disordering process that would modify the spin model. Firstly the very large mean squared displacement will

mean that the translational motions will contribute to the disorder, for example by allowing two molecules to move close to each other and altering their orientations in response, or allowing certain relative orientations to move two molecules further apart. Secondly, the importance of steric hindrance effects that arise from certain relative orientations has been pointed out (Coulon and Descamps 1980). The ordering of the low-temperature phase, or symmetrically related ordering, appears to give the only possible types of environments that an ordered molecule can reside in without the problems associated with steric hindrance. When a molecule rotates, it will always lead to steric hindrance interactions which within the sample can only be overcome by molecules adopting other types of orientations. Thus the ideal spin model cannot exist, and must be modified by the existence of other orientations. One can imagine such disordering occurring in the low-temperature phase just below the transition temperature in the vicinity of a molecule that has been given enough kinetic energy to allow it to rotate out of its potential well.

To summarise, the simulations have shown that real-space precursor ordering of the molecular orientations is not as straightforward as assumed in the discrete spin model, but precursor ordering of collective orientational variables in reciprocal space is dramatic. Expressed another way, although the system displays some incipient real-space ordering, the ordering processes are more clearly seen in reciprocal space through the large static couplings to the acoustic phonons and through the long-lived collective fluctuations at the appropriate points in the Brillouin zone.

6.3. Collective dynamics

This study has presented an analysis of the effects of the disorder and the rotation–translation coupling on the collective dynamics. Unfortunately it is not straightforward to correlate the results with experimental data (More and Fouret 1980, More *et al* 1984) as the available experimental data are primarily concerned with understanding the behaviour of fluctuations in one region of reciprocal space, or else are focused on the acoustic modes using constant-energy measurements. The only relevant data concern the linewidths of quasi-elastic scattering from unspecified modes with wave-vectors along $(1, 1, 1)$ around one region of wave-vector transfer Q. These data showed little wave-vector dependence of the linewidths, in contrast to many of the results presented here, which may suggest that the scattering was primarily associated with those orientational variables that are not coupled to acoustic phonons. It is not within the scope of this paper to calculate the expected neutron scattering cross sections for different collective modes, but by using the analysis given in the Appendix this would not be difficult to do. In fact, extensive calculations of predicted cross sections are essential preliminaries to any systematic neutron scattering experiment (Pawley 1972). It is hoped that the behaviour found in these simulations will be studied experimentally. Such studies may be able to examine the extent of the rotation–translation coupling for different modes along different symmetry directions.

6.4. Theoretical analysis

We summarise here both what we understand about the OD in CBr_4 and what needs a firmer theoretical foundation. Symmetry arguments have shown which modes are coupled. The model developed in the preceding section used various parameters that were obtained from the simulation (frequencies and coupling parameters) or from fitting

(the relaxation parameters), and was able to explain the nature of the dynamics of the collective variables. Thus we understand theoretically how the coupling affects the dynamic properties.

What remains is to be able to calculate the coupling parameters *ab initio*, starting from the model potential. This could be achieved by building upon the work of Michel and Naudts (1977, 1978), and we believe that similar work for CBr_4 is in progress (Fouret 1985). It is improbable, however, that the relaxation coefficients could be calculated, as these represent approximate anharmonic effects. This theoretical work should be able to identify the microscopic interactions that favour the coupling of the acoustic modes to the T_{2u} orientational variables over the T_{1u} variables and hence show why the observed low-temperature structure is the favoured one.

7. Conclusions

A computer simulation model of the OD phase of CBr_4 which was developed in I for the study of single-molecule real-space properties has been used to study collective properties. The form of the coupling between orientational variables and TA phonons has been calculated, and the collective dynamics have been studied. The effect of the coupling on the dynamics has been understood by using a model based on Mori theory, which has reproduced the most important feature that at large couplings the acoustic modes become relaxational with narrow frequency widths. The phase transition to the ordered phase has been discussed in light of the results obtained.

We have pointed out that more theoretical work is needed in order to explain the observed coupling in terms of the microscopic inter-molecular interactions in the crystal. However, it may be of greater importance to verify experimentally that the features of the collective modes observed in the simulations are also present in the real OD phase of CBr_4. The technique of coherent inelastic neutron scattering would be ideal for this, as has already been demonstrated (More and Fouret 1980), and to assist we have indicated the way in which the different correlation functions studied may contribute to any scattering cross section.

Appendix

We derive a form for the inelastic neutron scattering factor for OD crystals following the approach of Michel and Naudts (1978), adapted for neutral tetrahedral molecules. We consider here the intermediate scattering factor

$$G(\boldsymbol{Q}, t) = \int S(\boldsymbol{Q}, \omega) \, e^{-i\omega t} \, dt = \langle \rho(\boldsymbol{Q}, t)\rho(-\boldsymbol{Q}, 0)\rangle.$$

where the density operator $\rho(\boldsymbol{Q}, t)$ has been defined in § 5 as

$$\rho(\boldsymbol{Q}, t) = \sum_i b_i \exp(i\boldsymbol{Q} \cdot \boldsymbol{r}_i(t))$$

and r_i is the position vector of the ith atom, and b_i the corresponding scattering length r_i is expanded as

$$r_i(t) = R_i + u_i(t) + d_i(t)$$

where R_i is the equilibrium position of the molecular centre, $u_i(t)$ is the instantaneous displacement of the centre and $d_i(t)$ the instantaneous position of the atom with respect to the molecular position. We use the familiar spherical harmonic expansion for the bromine atoms:

$$\exp(\mathrm{i}Q \cdot d) = 4\pi \sum_{l=0}^{\infty} \sum_{m=-l}^{l} j_l(Qd) Y_{l,m}^*(Q) Y_{l,m}(d)$$

and retain only the terms for $l = 0, 3$. The $l = 3$ summation can be transformed to the orientational variables

$$\sum_{\mu=1}^{4} \sum_{m=-3}^{3} Y_{3m}^*(Q) Y_{3m}(d_\mu) = \sum_{\alpha=1}^{7} c_\alpha \hat{Y}_\alpha(Q) Y_\alpha$$

where $\hat{Y}_\alpha(Q)$ has a similar definition for a unit vector along Q as for Y_α. Values of the coefficients c_α, $\alpha = 1$–7, are

$$c_1 = c_2 = c_5 = 140/9\pi \qquad c_3 = c_4 = c_6 = c_7 = 35/18\pi.$$

Thus the density operator can be re-expressed:

$$\rho(Q, t) = \sum_i \exp(\mathrm{i}Q \cdot R_i) \exp(\mathrm{i}Q \cdot u_i(t)) \left(b_\mathrm{C} + b_\mathrm{B} \sum_{\mu=1}^{4} \exp(\mathrm{i}Q \cdot d_{i\mu}(t)) \right)$$
$$= \rho_0(Q, t) + \rho_3(Q, t)$$

where

$$\rho_0(Q, t) = (b_\mathrm{C} + 4b_\mathrm{B} j_0(Qd)) \sum_i \exp(\mathrm{i}Q \cdot R_i) \exp(Q \cdot u_i(t))$$

$$\rho_3(Q, t) = 4\pi b_\mathrm{B} j_3(Qd) \sum_i \exp(\mathrm{i}Q \cdot R_i) \exp(\mathrm{i}Q \cdot u_i(t)) \sum_{\alpha=1}^{7} c_\alpha \hat{Y}_\alpha(Q) Y_\alpha$$

and b_c and b_B are the scattering lengths for the carbon and bromine atoms respectively. The intermediate scattering factor can therefore be expanded:

$$G(Q, t) = \langle \rho_0(Q, t) \rho_0(-Q, 0) \rangle + \langle \rho_3(Q, t) \rho_0(-Q, 0) \rangle + \langle \rho_0(Q, t) \rho_3(-Q, 0) \rangle$$
$$+ \langle \rho_3(Q, t) \rho_3(-Q, 0) \rangle$$
$$= G_{00}(Q, t) + G_{30}(Q, t) + G_{03}(Q, t) + G_{33}(Q, t).$$

The acoustic mode component, $G_{00}(Q, t)$, can be treated in the usual manner. Noting that the Debye–Waller factor $W(Q)$ is given as

$$W(Q) = \langle (Q \cdot u(0))^2 \rangle / 2$$

and by transforming to collective coordinates, we obtain

$$G_{00}(Q, t) = (b_\mathrm{C} + 4b_\mathrm{B} j_0(Qd))^2 \, \mathrm{e}^{-2W(Q)} Q_\beta Q_\gamma \langle u_\beta(k, t) u_\gamma(-k, 0) \rangle$$

where the summation over the cartesian indices $\beta, \gamma = 1, 2, 3$ is implied and it is assumed that $Q = k +$ Bragg vector.

The cross-terms simply follow as

$$G_{30}(\boldsymbol{Q}, t) = \left(b_{\mathrm{C}} + 4b_{\mathrm{B}}j_0(Qd)\right)4\pi b_{\mathrm{B}}j_3(Qd)\,\mathrm{e}^{-2W(\boldsymbol{Q})}Q_\beta \sum_{\alpha=1}^{7} \tilde{Y}_\alpha(\boldsymbol{Q})\langle Y_\alpha(\boldsymbol{k}, t)u_\beta(-\boldsymbol{k}, 0)\rangle c_\alpha$$

$$G_{03}(\boldsymbol{Q}, t) = \left(b_{\mathrm{C}} + 4b_{\mathrm{B}}j_0(Qd)\right)4\pi b_{\mathrm{B}}j_3(Qd)\,\mathrm{e}^{-2W(\boldsymbol{Q})}Q_\beta \sum_{\alpha=1}^{7} \tilde{Y}_\alpha(\boldsymbol{Q})\langle u_\beta(\boldsymbol{k}, t)Y_\alpha(-\boldsymbol{k}, 0)\rangle c_\alpha.$$

Finally the orientation–orientation correlation function is given by

$$G_{33}(\boldsymbol{Q}, t) = \left(4\pi b_{\mathrm{B}}j_3(Qd)\right)^2 \mathrm{e}^{-2W(\boldsymbol{Q})} \sum_{\alpha=1}^{7} \sum_{\alpha'=1}^{7} \tilde{Y}_\alpha(\boldsymbol{Q})\tilde{Y}_{\alpha'}(\boldsymbol{Q})\langle Y_\alpha(\boldsymbol{k}, t)Y_{\alpha'}(-\boldsymbol{k}, 0)\rangle c_\alpha c_{\alpha'}.$$

Note added in proof. The vanishing of the rotation–translation coupling parameters at $\boldsymbol{k} = 0$ as observed in the present study (§ 3), with maxima at the zone boundaries, is consistent with the recent predictions of Michel and Rowe (1985) for non-centrosymmetric molecules.

References

Coulon G and Descamps M 1980 *J. Phys. C: Solid State Phys.* **13** 2847
Cowley R A 1980 *Adv. Phys.* **29** 1
Dolling G, Powell B M and Sears V F 1979 *Mol. Phys.* **37** 1859
Dove M T 1986 *J. Phys. C: Solid State Phys.* **19**
Dove M T, Heilmann I U, Kjems J K, Kurittu J and Pawley G S 1983 *Phys. Status Solidi* **120**b 173
Dove M T, Pawley G S, Dolling G and Powell B M 1986 *Mol. Phys.* **57** 865
Fouret R 1985 private communications
Lynden-Bell R M, McDonald I R and Klein M L 1983 *Mol. Phys.* **48** 1093
Michel K H 1981 *Phys. Rev.* B **24** 3998
Michel K H and Naudts J 1977 *J. Chem. Phys.* **67** 547
—— 1978 *J. Chem. Phys.* **68** 216
Michel K H and Rowe J H 1985 *Phys. Rev.* B **32** 5818
More M 1982 *PhD Thesis* University of Lille
More M and Fouret R 1980 *Discuss. Faraday Soc.* **69** 75
More M, Lefebvre J and Hennion B 1984 *J. Physique* **45** 303
More M, Lefebvre J, Hennion B, Powell B M and Zeyen C M E 1980 *J. Phys. C: Solid State Phys.* **13** 2833
Parlinski K and Michel K H 1984 *Phys. Rev.* B **29** 396
Pawley G S 1972 *Proc. Symp. Neutron Inelastic Scattering (Vienna) 1972* (Vienna: IAEA) p 175
Pawley G S and Thomas G 1982 *J. Comput. Phys.* **47** 165
Pick R 1984 private communication
Powell B M, Dolling G and Nieman H F 1983 *J. Chem. Phys.* **79** 982
de Raedt B and Michel K H 1980 *Discuss. Faraday Soc.* **69** 88
Rowe J M, Rush J J, Chesser N J, Michel K H and Naudts J 1978 *Phys. Rev. Lett.* **40** 455
Rowe J M, Rush J J, Vagelatos N, Price D L, Hinks D G and Susman S 1975 *J. Chem. Phys.* **62** 4551